FLORIDA STATE UNIVERSITY

Extraction of Nanorod Projection Lengths from Scanning Electron Micrographs

Tanmoy Das

Committee Members:

Dr. Abhishek K. Shrivastava, Dr. Chiwoo Park, Dr. Arda Vanli

Master's Thesis Defense Presentation

09 July, 2015

Outline

- Objective & Problem Statement
- Present status of the problem
- Proposed Approach
- Evaluate Performance
- Summary

Introduction (Sec 1.1)

Nanorod: A nano-object whose size varies from 1-200 nm in two dimensions, and has aspect ratio (length divided by width) of 3 or larger.

Nanorod Array: An ordered arrangement of nanorods

Nanorod arrays have several applications:

- Cancer cell destruction [2]
- Display technology [3]
- Imaging system without lens [7]

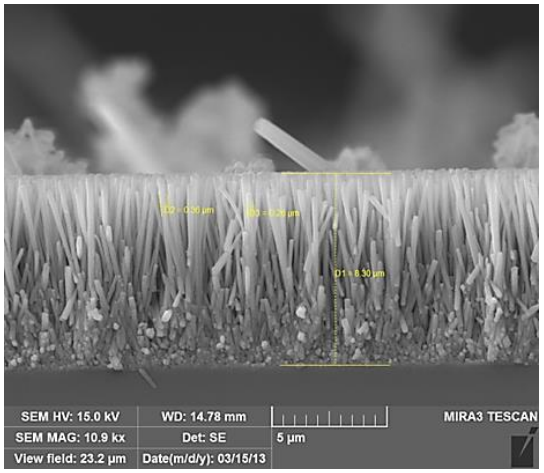

Fig 1.1: SEM image of AZO nanorod array [1]

Dimension Estimation is Key! (Sec 1.1)

- Nanomaterial properties are strongly correlated to nano-object dimensions in many applications
- Example: Filters in indoor air purifiers
  - Efficiency of filter depends on dimension and arrangement of nanowires in it

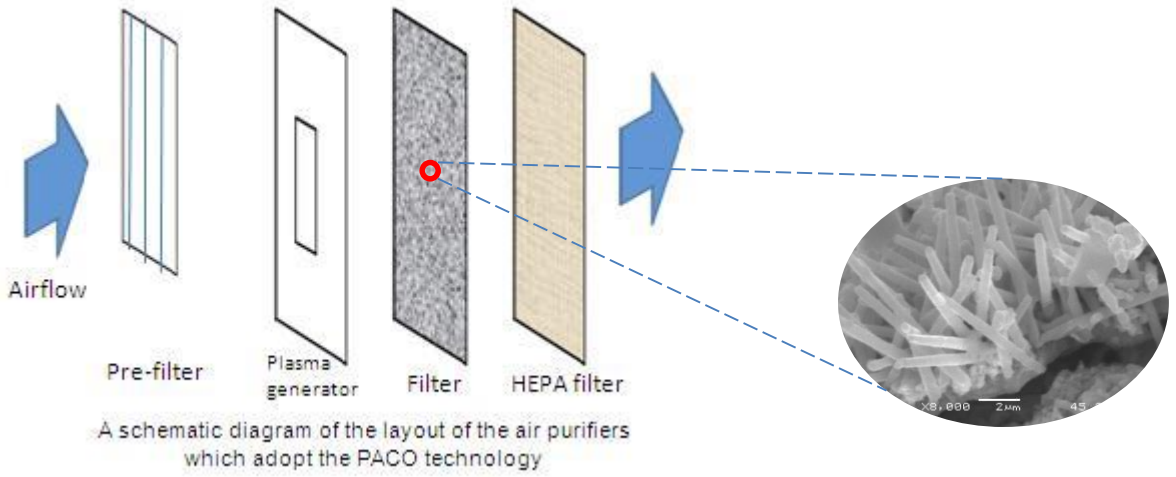

* Courtesy: Dr. Oscar K. S. Hui, Hanyang University

Fig 2: Filter in purifier

Aim of the Research (Sec 1.1)

- Estimate dimensions of nanorods in a nanorod array using electron micrograph

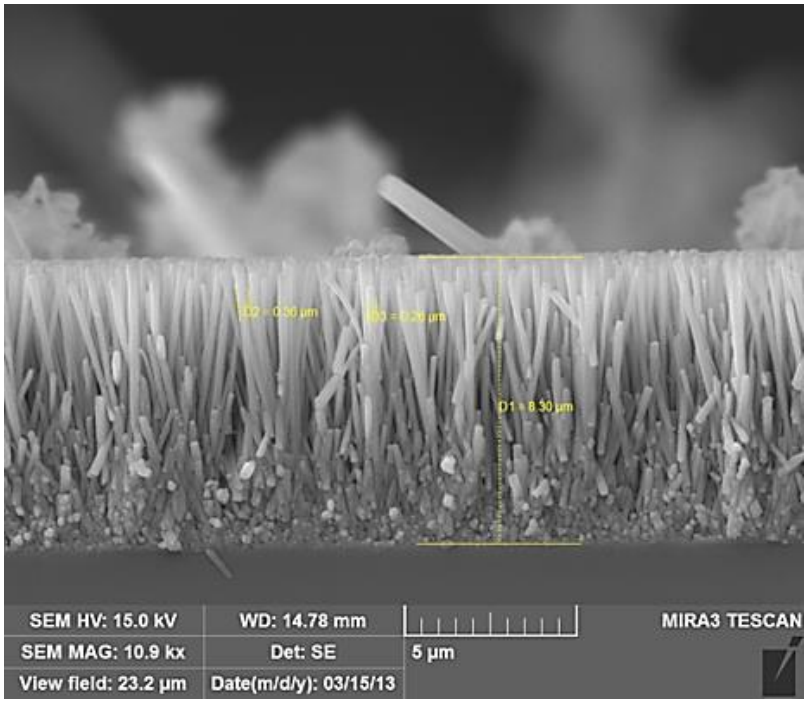

Fig 1.1: SEM image of AZO nanorod array [1]

Challenges in Length Estimation (Sec 1.2)

1. Each electron micrograph shows nanorod *projections*
   - Projection estimates *cannot* be used as length estimates
2. Extracting projections from an EM ➡ Objective of this Thesis
   - Usually done manually – slow and prone to human error

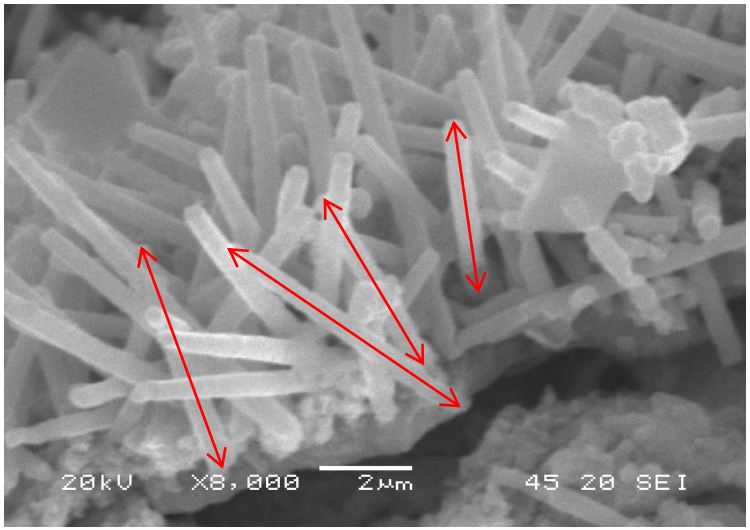

Fig2(a). SEM image of Co_3O_4 nanowires

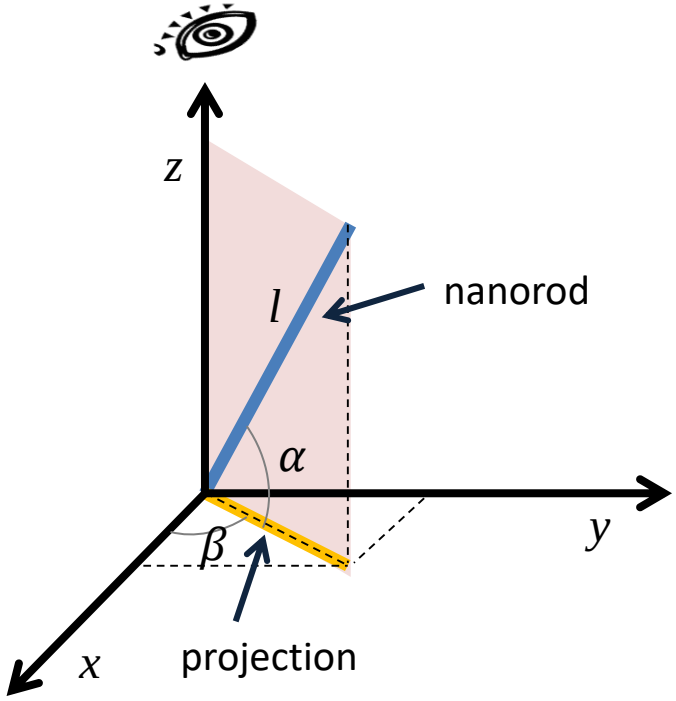

Fig 1.2: Projection of nanorods

Problem Statement (Sec 1.2)

Extraction of Nanorod Projection Lengths from Electron Micrographs

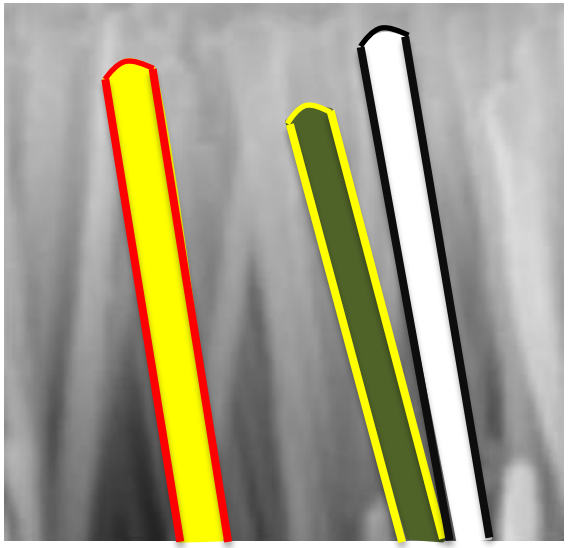

Fig 3: Nanorods with projections

Expected Contribution of the Research (Sec 1.2)

- Contributing to dimensional quality engineering of nanorod manufacturing
- Automatic identification of nanorods
- Save computational time of researchers
- Reduce error of manual identification of nanorods

Related Literature Review

- Image Segmentation (Sec 2.1):
  - Edge detection – Sobel [50], Canny [17]
  - Region based segmentation [36]
  - Graph based methods - Min cut [107], Normalized cut [91]
  - Snake/ Active contours [58]

- Template Matching (Sec 2.2):
  - Correlation based particle detection [85]
  - Geometric feature based [68]

Related Literature Review

- Approaches for Overlapping Particles (Sec 2.3):
  - Segmentation, inference, and classification [79]
  - Separating touching and overlapping particle [53]

- Discussion (Sec 2.4):
  - None of existing algorithms are able to extract nanorods from electron micrographs
  - Overlapping particles is the main reason why existing algorithms do not work well.

Challenges

1. Low signal-to-noise ratio
2. High overlap among nanorods

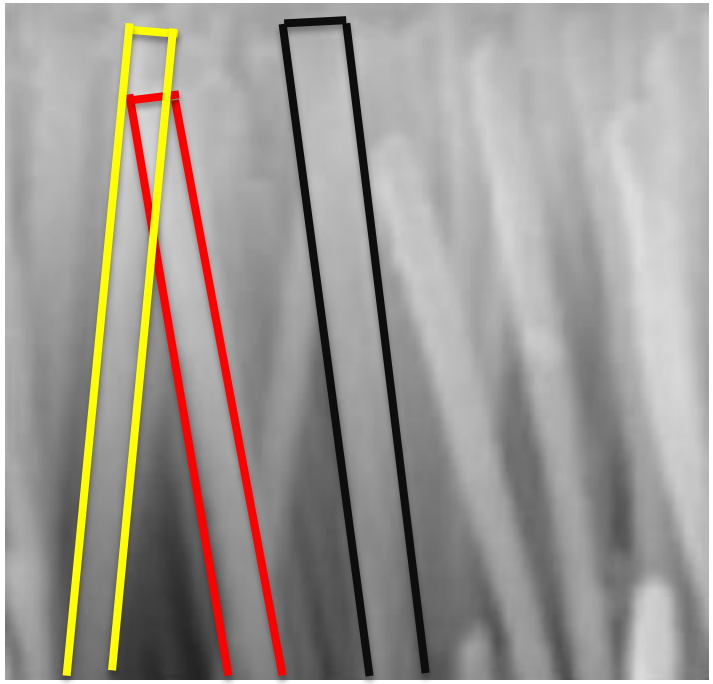

Fig 3: Illustration of overlap

Proposed Approach: Decomposing the Problem (Sec 3.1)

- Since we're interested *only* in nanorod projections, we only consider segmenting out 'heads' of nanorods.
- Extrapolate those heads to the substrate.

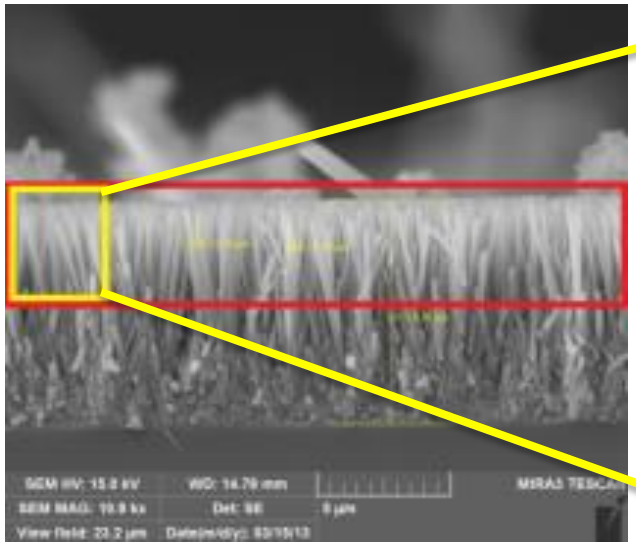

Fig 3.5(a): Original input image

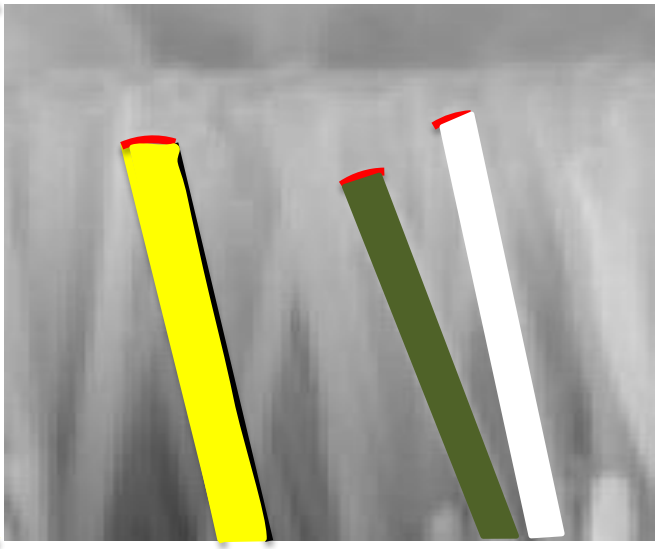

Fig 3.5(b) Cropped image

Develop an algorithm which can extract nanorod heads

Proposed Algorithm to Extract Nanorod Heads (Sec 3.2)

1. Preprocessing
2. Identifying Top Edges
3. Estimating Side Edges
   - Fit robust regression to side edge data
   - Connect edges based on slope difference
   - Dilate Side edges
4. Edge-to-nanorod association
   - Find nanorod candidates by finding intersections of left, top, and right edge segments
   - Identify nanorods from candidate nanorods
5. Estimating Projection Length

Illustrating Example: Preprocessing (Sec 3.2.1)

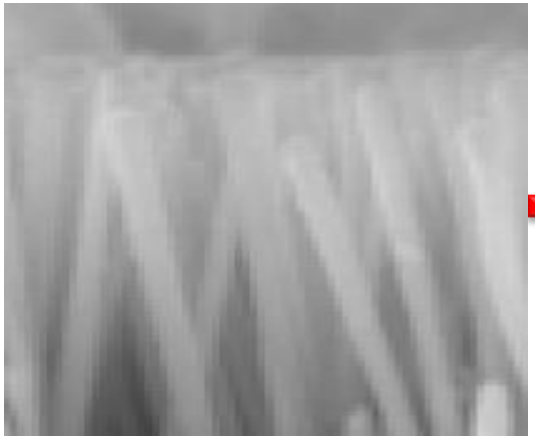

Fig 3.6(a): Section of SEM image

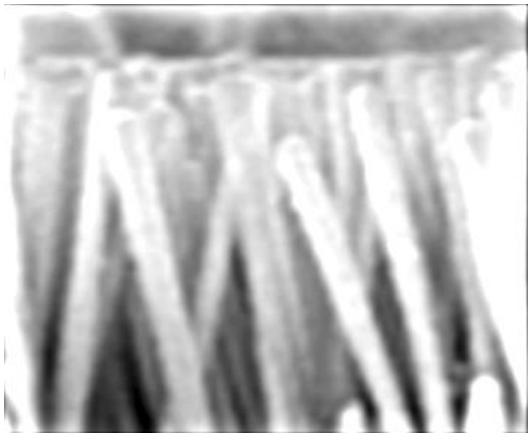

3.6(b): Preprocessed Image

- Apply Gaussian filter

$$G(x,y) = \frac{1}{2\pi\sigma^2} . e^{-\frac{x^2+y^2}{2\sigma^2}}$$

- Sharpen the image

Identifying *Top* Edges (Sec 3.2.2)

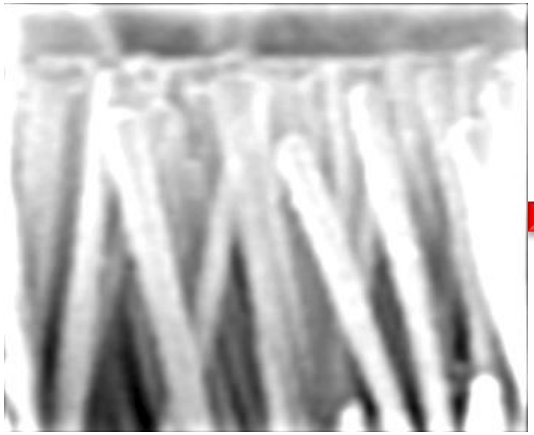

Fig 3.6(b): Preprocessed Image

3.6(c): All top edges
3.6(c): Final top edges

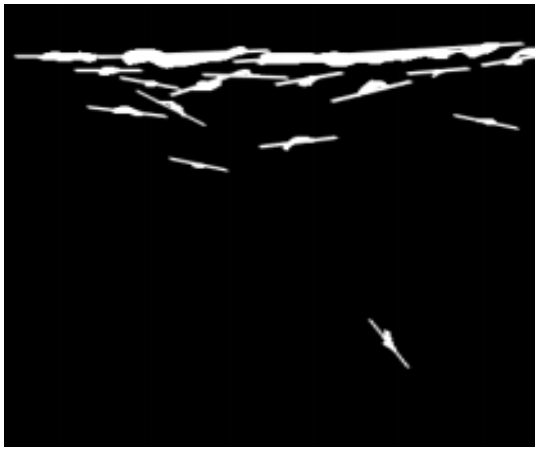

3.6(d): Top edge after dilation

- Convolve the preprocessed image with Gradient of Gaussian in Y direction
- Delete small components

$Th_{min.cc.top} = \varepsilon * \mathrm{E}[\text{width of nanorod}]$

- Dilate the detected top edges

$$Th_{dilate.top} = \frac{1}{2}(1-\varepsilon) * (\#\text{ of pixels in top edge})$$

Fig 6

Estimating *Side* Edges: Obtain Side Edges (Sec 3.2.3)

Fig 3.7(a) Edges for Fig 3.6(b)

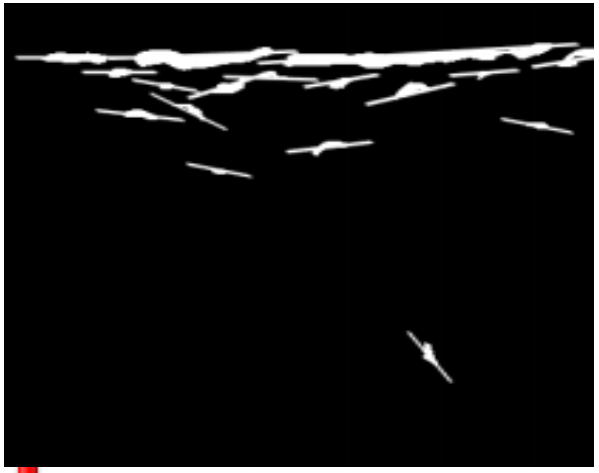

3.6(d): Top edge after dilation

- Apply Canny to preprocessed image

$$G = \sqrt{(G_x^2 + G_y^2)}$$

$$\theta = atan(G_x, G_y)$$

- Fit robust regression
  - $Th_{min.cc.side.fit}$
  - $Th_{theta.side}$

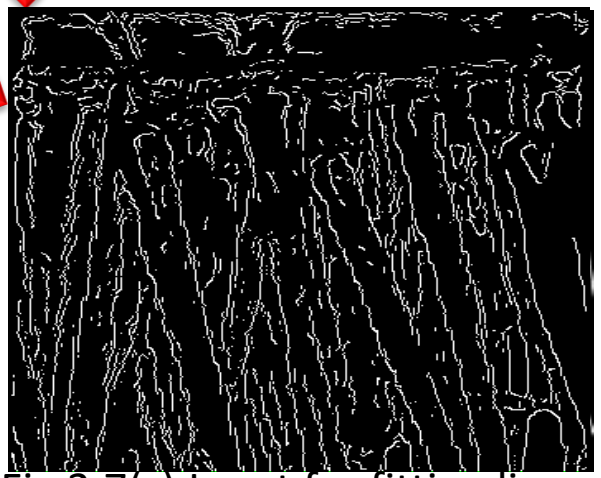

Fig 3.7(c) Input for fitting line

Fig 3.7(c) All edges & top edges

Fig 3.7(c) Side edges after fitting line

Estimating *Side* Edges: Merging & Dilating (Sec 3.2.3)

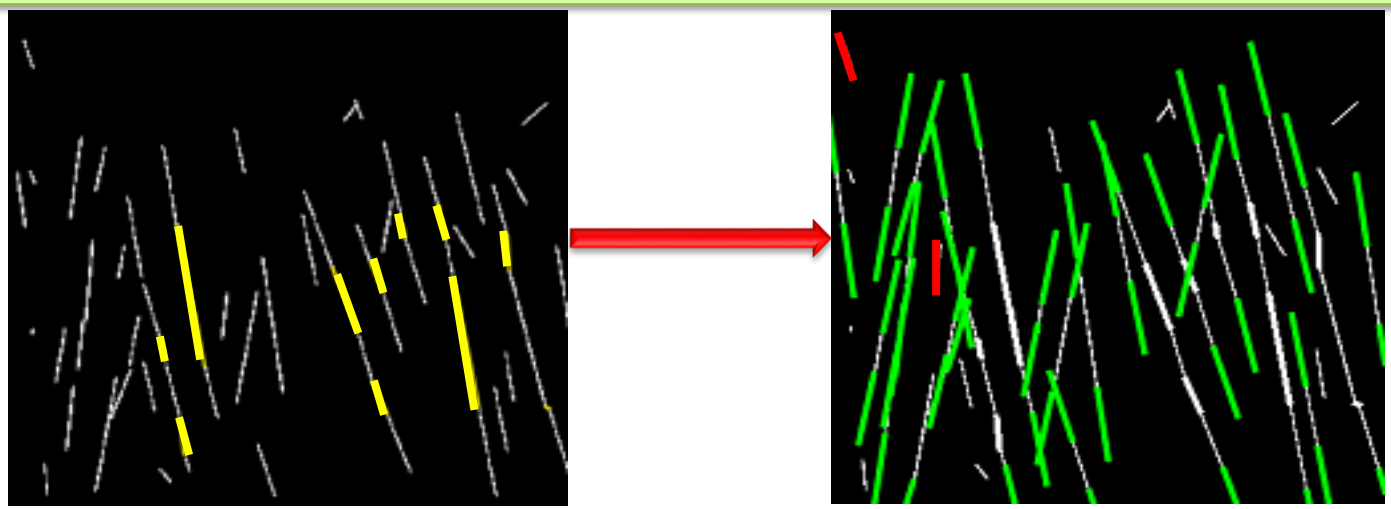

Fig 3.8(a) Merge side edges

Fig 3.8(b) Dilation of side edges

- Merge side edges

  $Th_{dist.grad}$

  $Th_{dist.grad.normal}$ = width of nanorod/4

  $Th_{\Delta slope.side} = 5°$

- Dilate side edges

  $Th_{length.side} = 25$ pixels

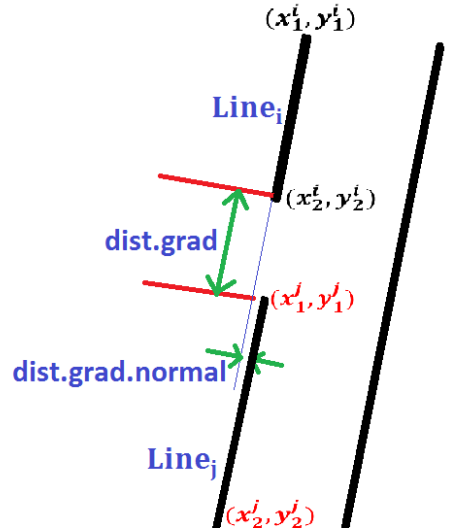

(c) Condition to merge two side edges

Edge-to-nanorod Association (Sec 3.2.4)

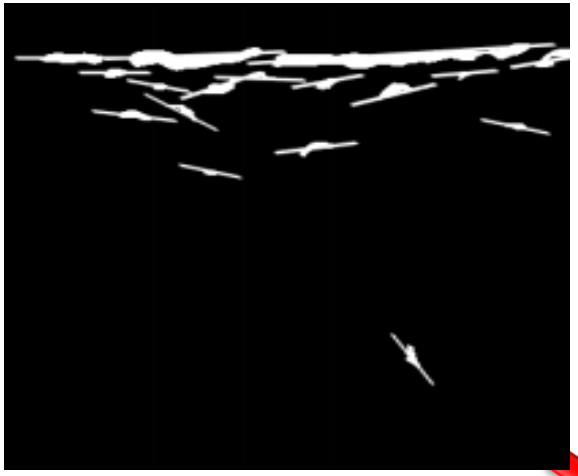

3.6(d): Top edges after dilation

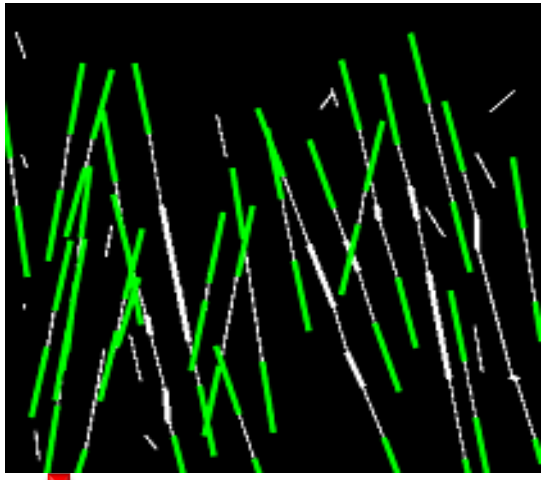

3.8(b) Dilation of side edges

- Find intersection between top edges & side edges

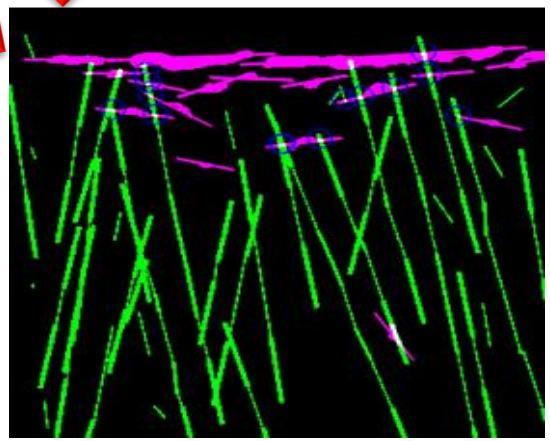

Fig 3.9 (a) Top edge & side edge intersections

Edge-to-nanorod Association (Sec 3.2.4)

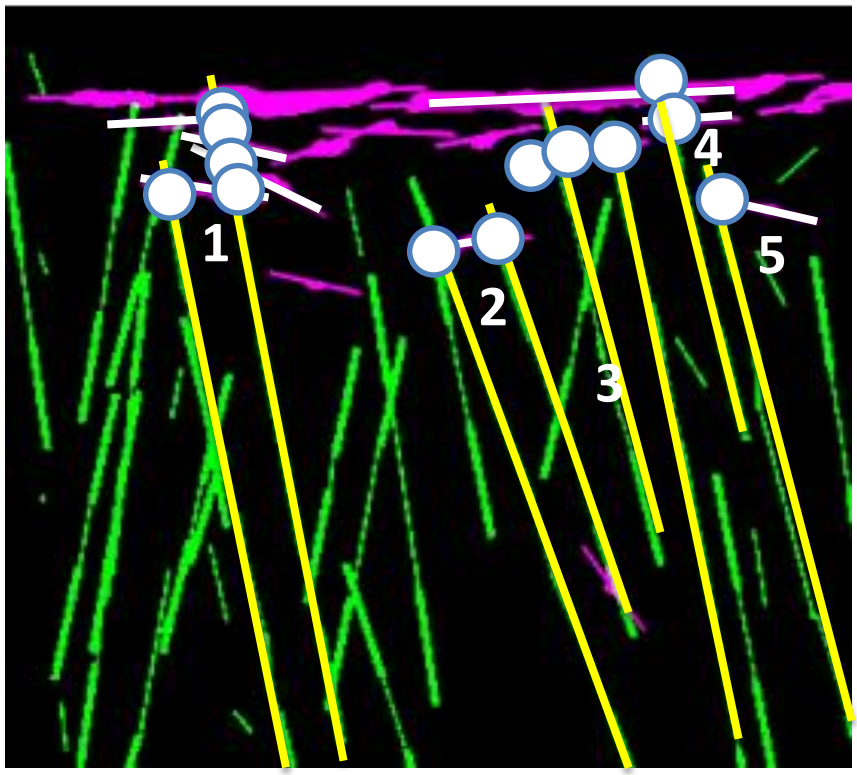

Fig 3.9(a) Candidate nanorods

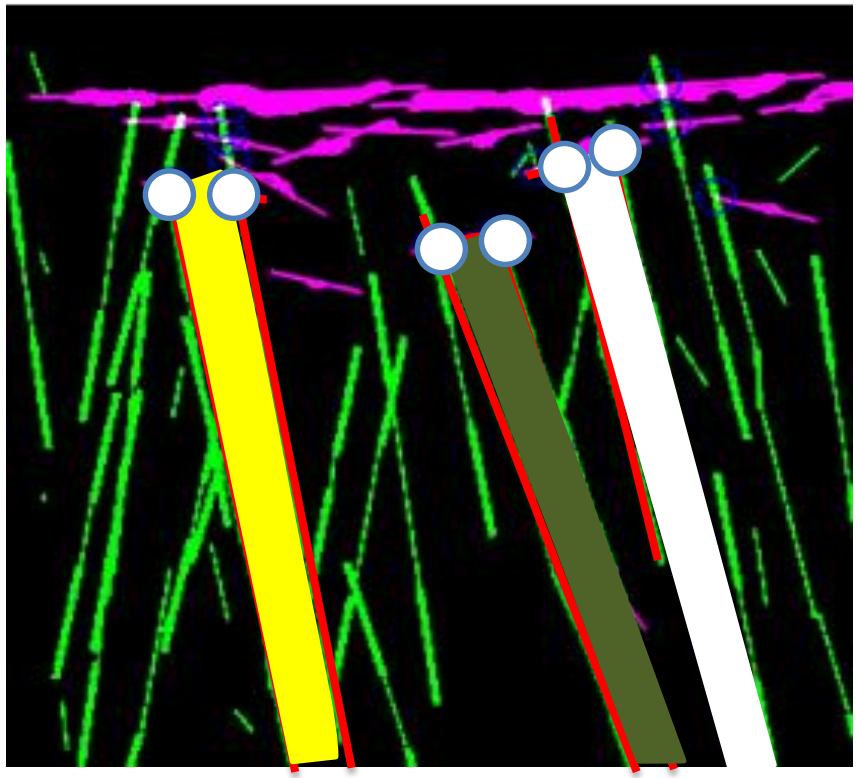

Fig 3.9(b) Final extracted nanorods

- Obtain candidate nanorods (Based on intersection points, list edges)
- Clean false nanorods

Estimating Projection Lengths (Sec 3.2.5)

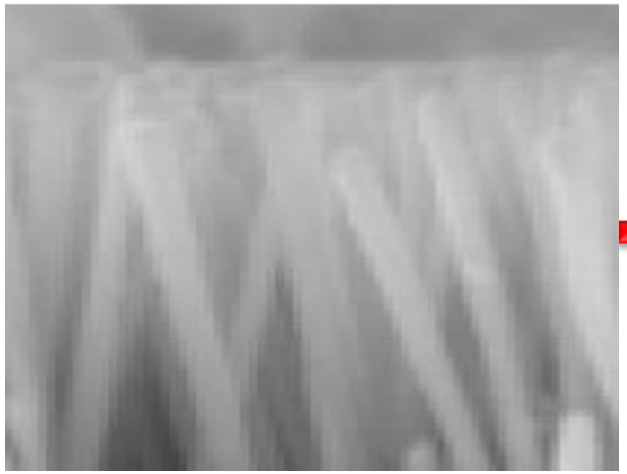

Fig 3.10(a) Input image

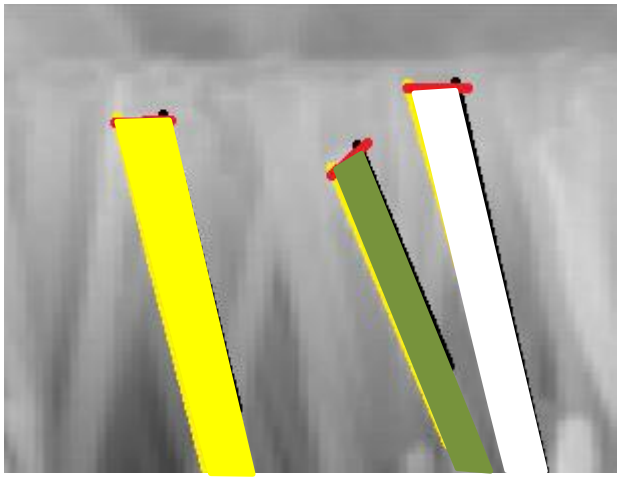

Fig 3.10(b) Final Nanorods

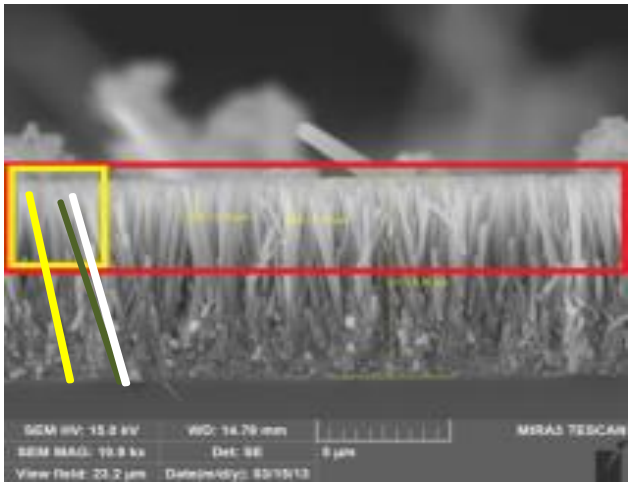

Fig 3.10(c) Original input image with projection lengths

Flowchart

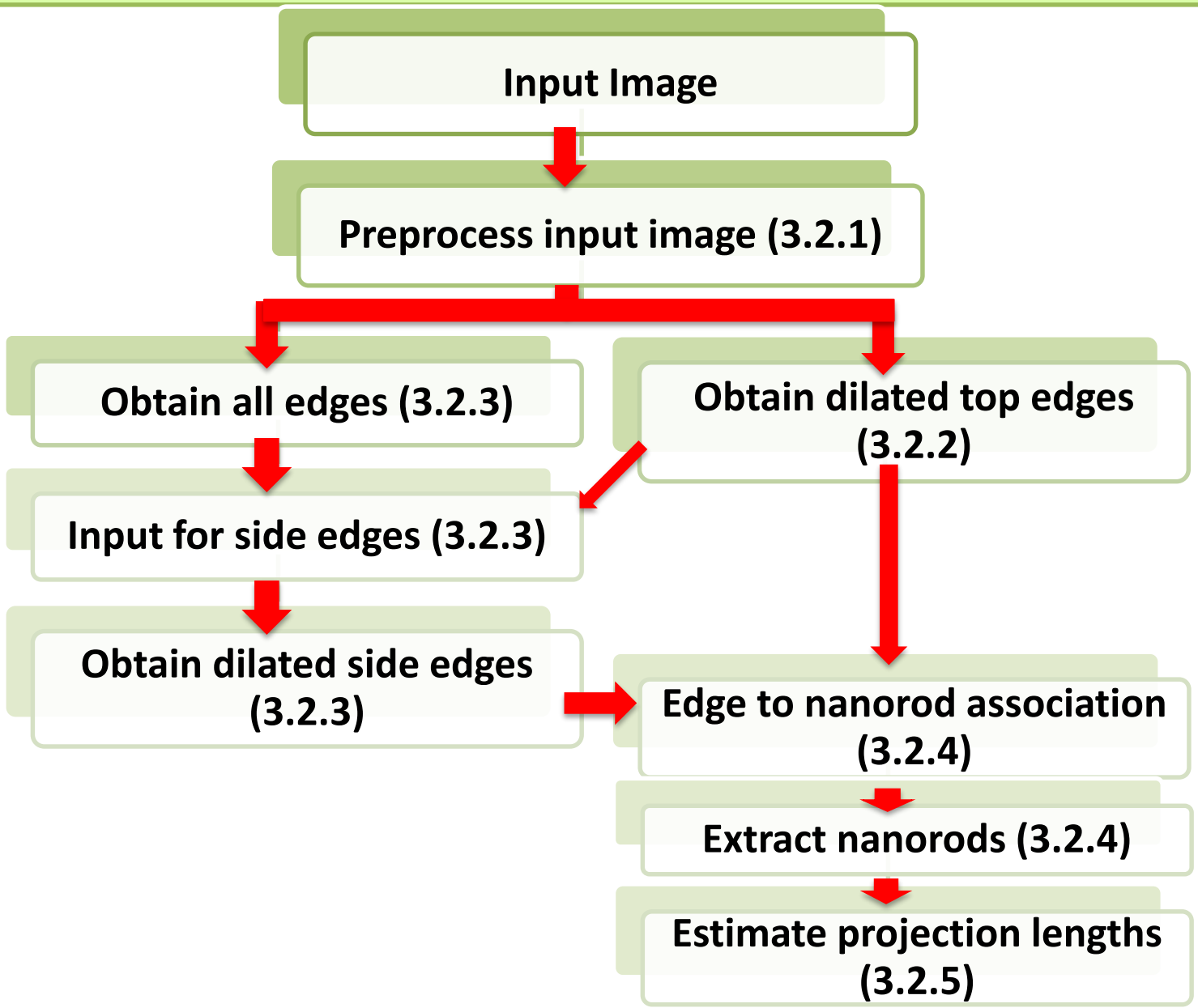
Input Image
Preprocess input image (3.2.1)
Obtain all edges (3.2.3)
Obtain dilated top edges (3.2.2)
Input for side edges (3.2.3)
Obtain dilated side edges (3.2.3)
Edge to nanorod association (3.2.4)
Extract nanorods (3.2.4)
Estimate projection lengths (3.2.5)

Evaluate Performance

- **Data for Experimentation (Sec 4.1)**
  - Input Data
  - Ground Truth

Data for Experimentation (Sec 4.1)
Input Image (medium degree of overlap)

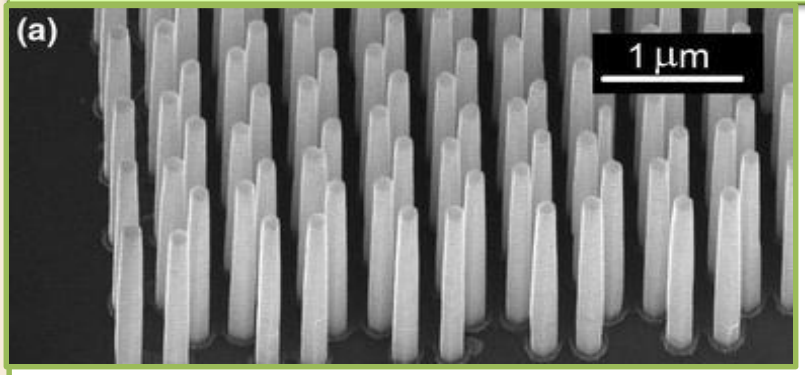

Fig 4.1(a) **Image 1** [102]

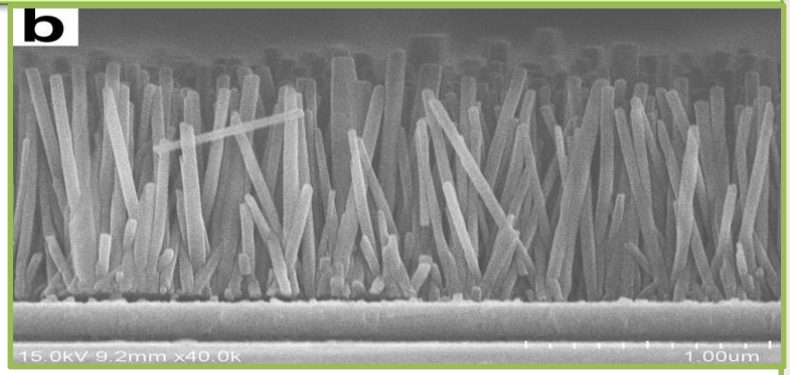

Fig 4.1(b) **Image 2** [64]

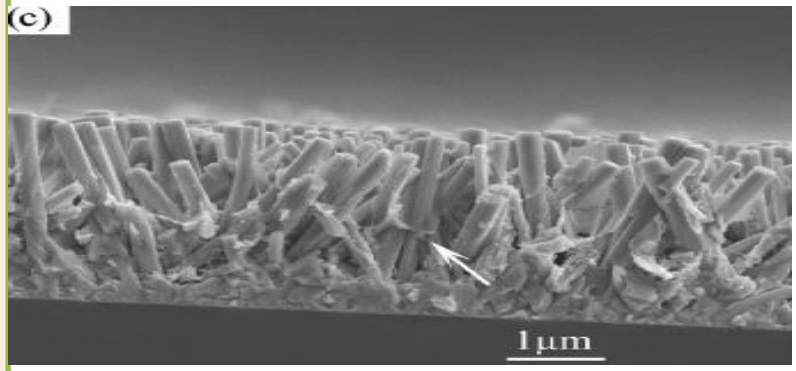

(c) **Image 3** [31]

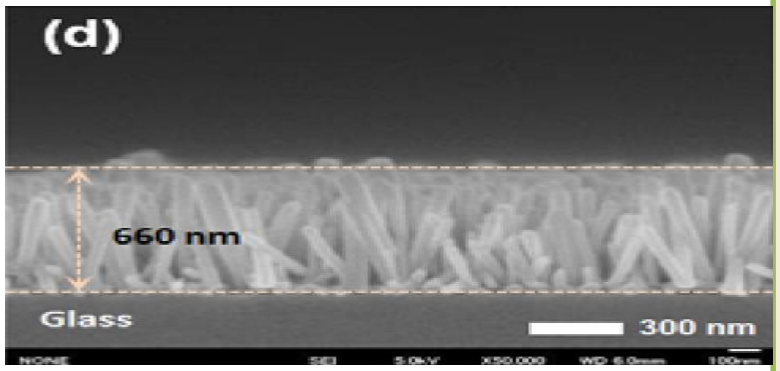

(d) **Image 4** [52]

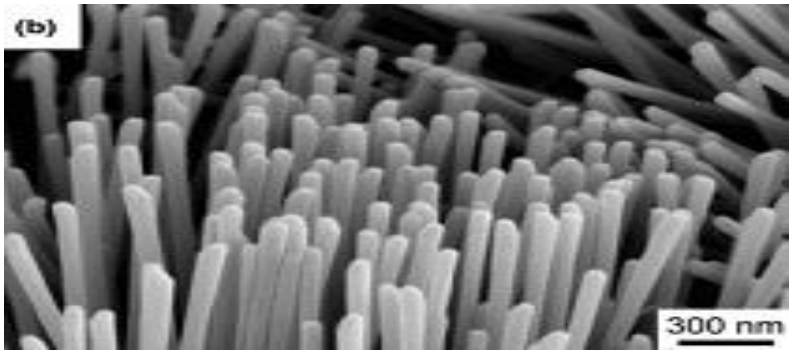

Fig 4.1(e) **Image 5** [66]

Data for Experimentation (Sec 4.1)
Input Image (high degree of overlap)

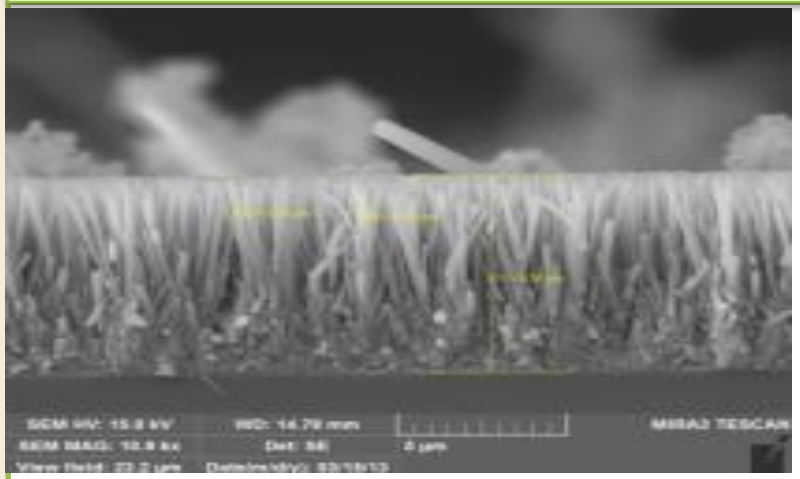

Fig 4.3(a) **Image 6** [86]

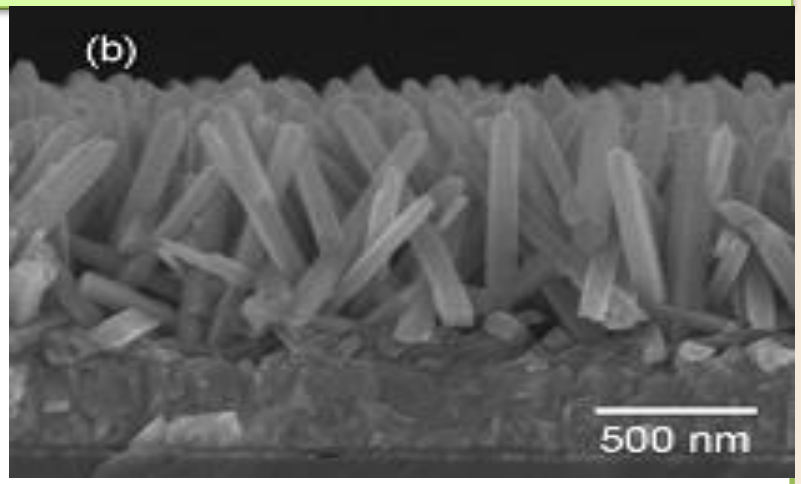

Fig 4.3(b) **Image 7** [65]

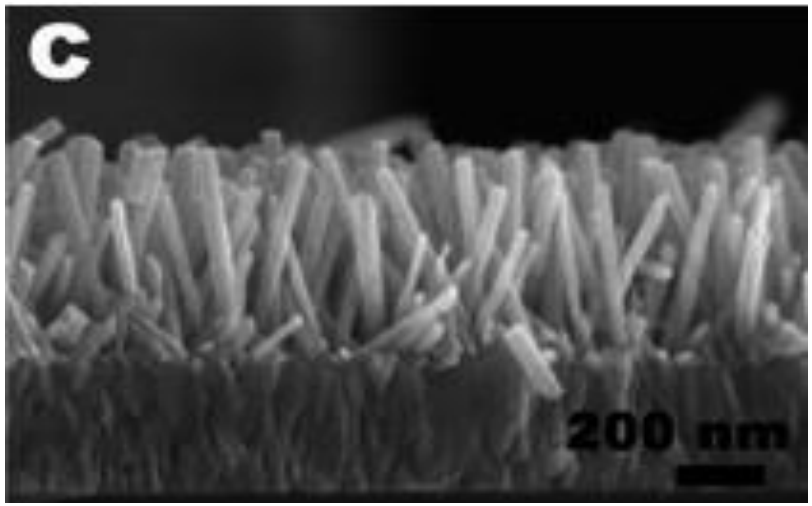

Fig 4.3(c) **Image 8** [104]

Performance Metrics (Sec 4.2)

01: Evaluate the number of nanorods detected

x = The number of nanorods detected by the algorithm,

y = The number of false alarms/detections.

N = The total number of nanorods exist in the image. (N is calculated from ground truth image)

02: Evaluate the projection length

Mean Square Error,

$$MSE = \frac{\sum_{i=1}^{x}(L_{actual} - L_{estimated})^2}{x}$$

$L_{estimate}$ = The estimated projection length of a particular nanorod,

L_{actual} = The actual projection length of a particular nanorod.

Performance Metrics (Sec 4.2)

	Image	The number of true nanorods, N	The number of truly detected nanorods by the algorithm, x	The number of false detection, y	MSE
1	Image 1	27	5	0	0.015
2	Image 2	74	13*	3*	0.1
3	Image 3	35	11	5	1.1
4	Image 4	34	8*	3*	1.02
5	Image 5	42	5	3	0.2
6	Image 6	40	14	1	2
7	Image 7	41	10*	1	0.7
8	Image 8	36	17	3	0.8

***Updated**

Output of Proposed Algorithm (Sec 4.3)

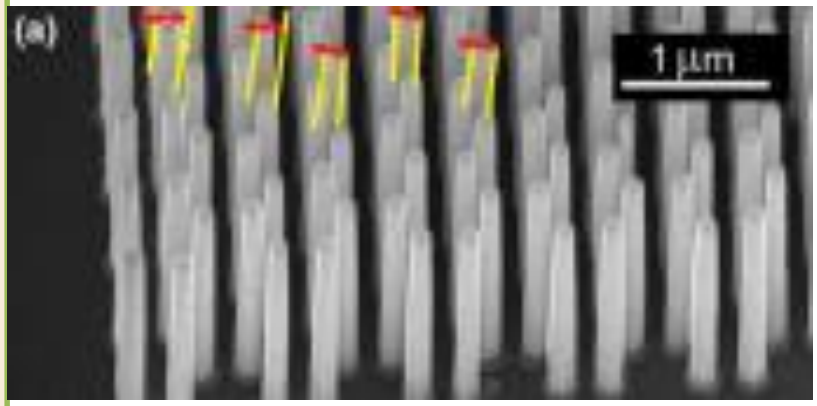

Fig 4.7(a) Output for Image 1

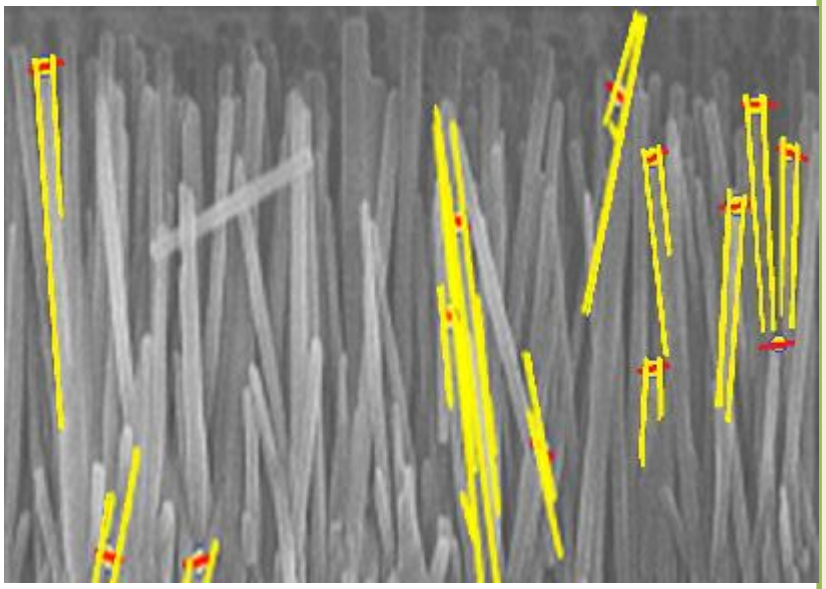

Fig 4.7(b) Output for Image 2

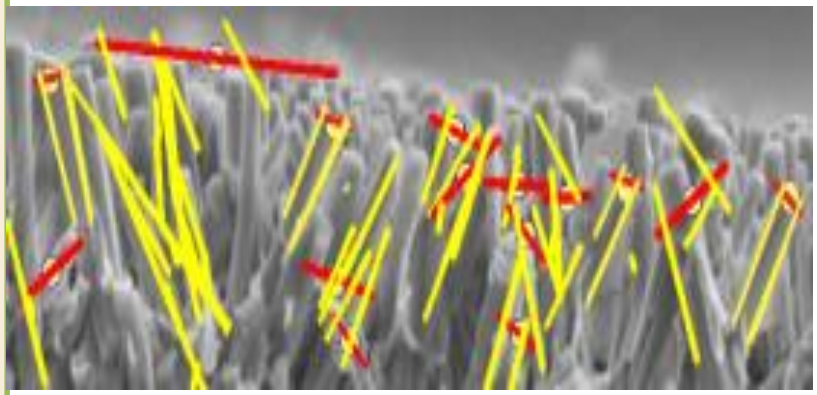

Fig 4.7(c) Output for Image 3

Output of Proposed Algorithm (Sec 4.3)

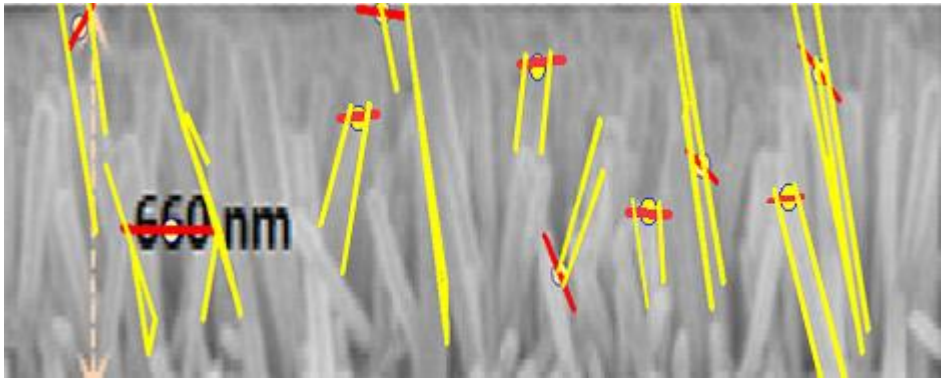

Fig 4.8(b): Output for Image 4

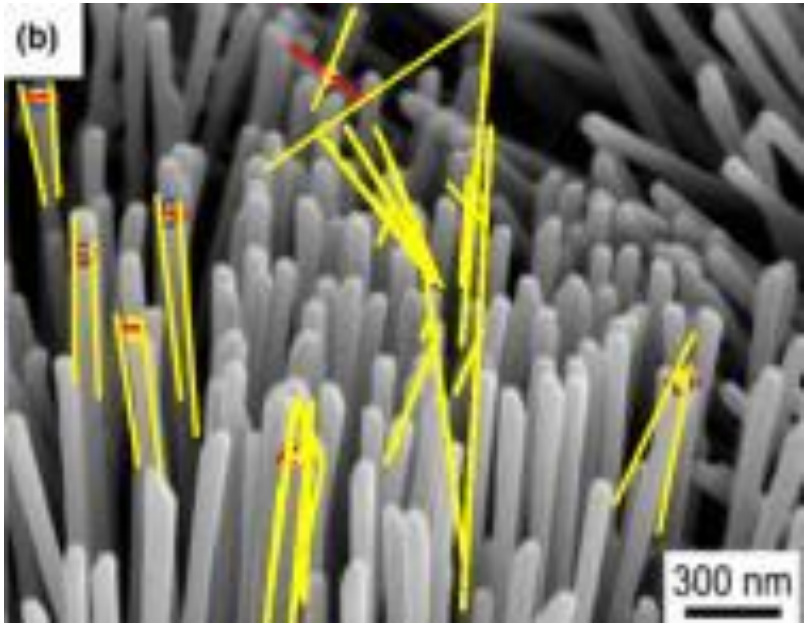

Fig 4.8(a): Output for Image 5

Output of Proposed Algorithm (Sec 4.3)

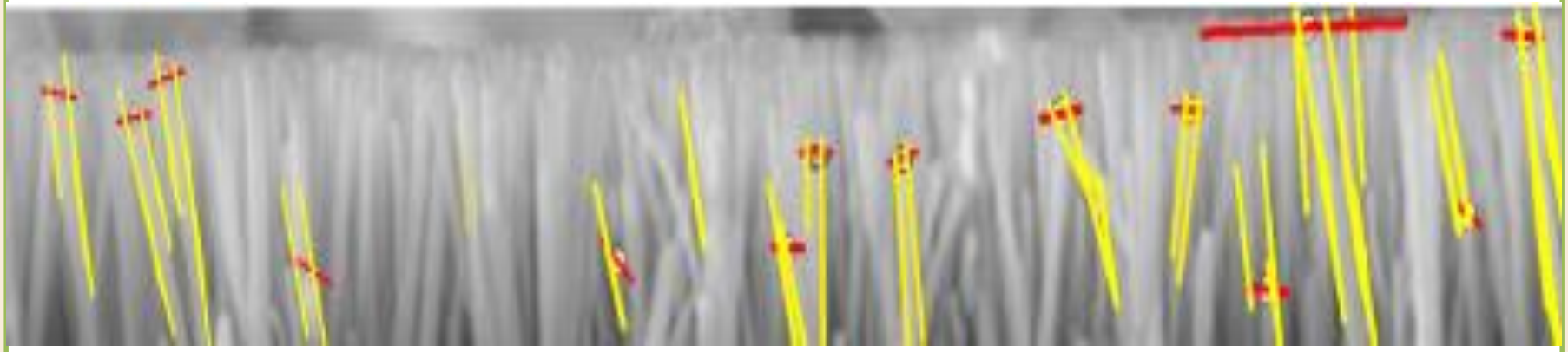

Fig 4.9(a) Output for Image 6

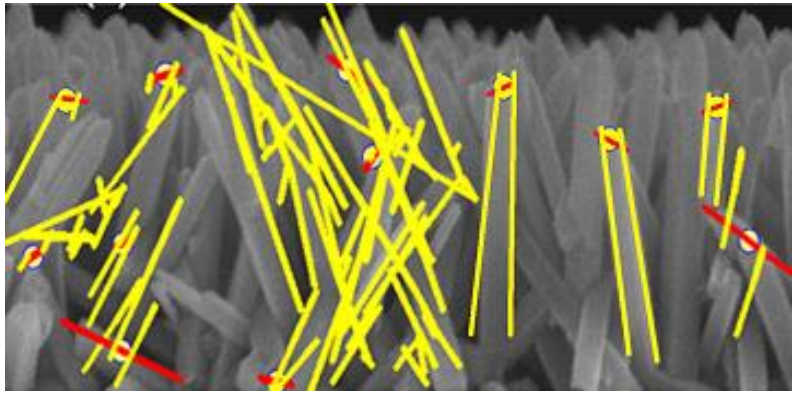

Fig 4.9(b) Output for Image 7

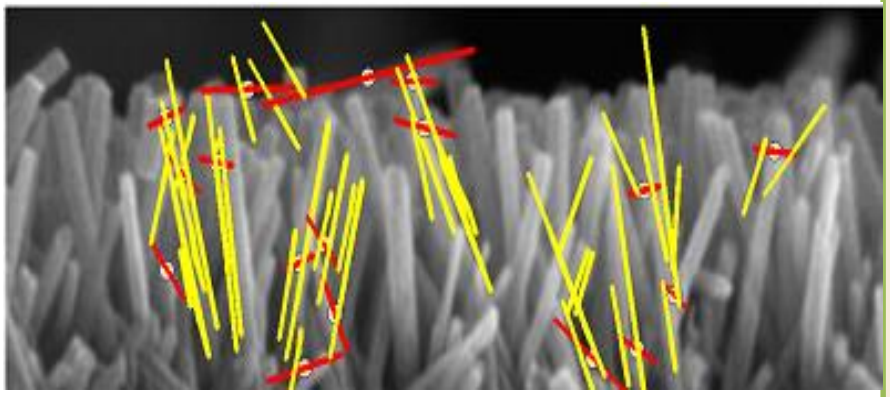

Fig 4.9(c) Output for Image 8

Compare the algorithm with other relevant algorithm (Sec 4.3)

- Compare the algorithm with other relevant algorithm
  - N-cut*
  - Snake**

* Normalized Cut Segmentation Code, Timothee Cour, Stella Yu, Jianbo Shi. Copyright 2004 University of Pennsylvania, Computer and Information Science Department.

** http://www.shawnlankton.com/2008/04/active-contour-matlab-code-demo/, 2008

Outputs of N cut

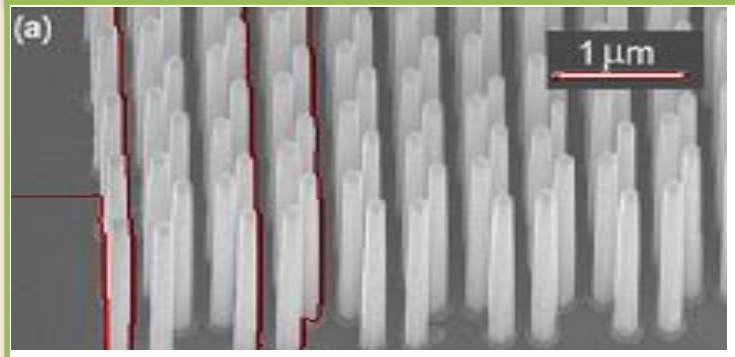

Fig 4.10(a): Image 1

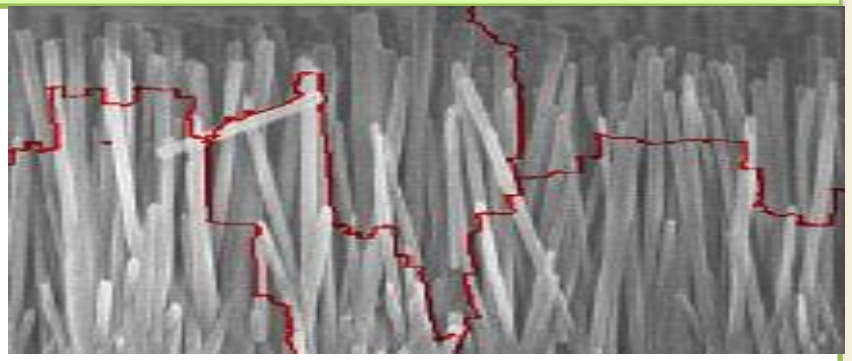

Fig 4.10(b): Image 2

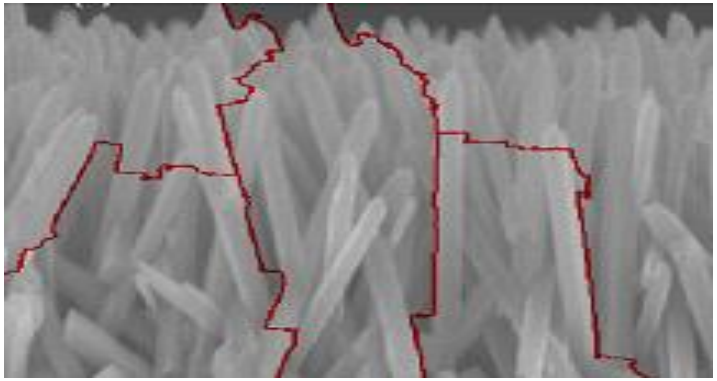

Fig 4.10(c): Image 3

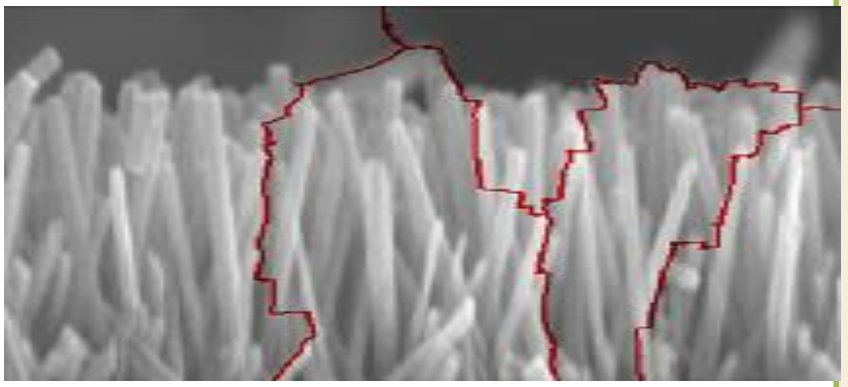

Fig 4.10(d): Image 4

Outputs of Snake

Fig 4.13(a): Image 1

Fig 4.13(b) Image 2

Fig 4.13(c) Image 3

Fig 4.13(d) Image 4

Summary (Sec 5.1)

- We have presented an automatic particle detection algorithm
  - Extract projection length of nanorods from Electron Micrograph
- Performance to extract nanorods from electron micrograph is better than existing algorithms.
- A contribution to dimensional quality engineering
  - Actual dimensions can be measured by combining projection lengths of multiple views.
- Challenges: Low Signal to noise ratio, high degree of overlap

Future Plan (Sec 5.2)

- Optimize the parameter values to improve the performance of the proposed algorithm
- Determine the actual lengths of nanorods

Reference

[2] Kuo-Wei Hu, Tzu-Ming Liu, Kuei-Yi Chung, Keng-Shiang Huang, Chien-Tai Hsieh, Chi-Kuang Sun, and Chen-Sheng Yeh. Ecient near-ir hyperthermia and intense nonlinear optical imaging contrast on the gold nanorod-in-shell nanostructures. Journal of the American Chemical Society, 131(40):14186-14187, 2009.

[3] Mihail C Roco. Nanoparticles and nanotechnology research. Journal of Nanoparticle Research, 1(1):1-6, 1999.

[4] Abrin L Schmucker, Nadine Harris, Matthew J Banholzer, Martin G Blaber, Kyle D Osberg, George C Schatz, and Chad A Mirkin. Correlating nanorod structure with experimentally measured and theoretically predicted surface plasmon resonance. ACS nano, 4(9):5453-5463, 2010.

[5] Babak Sadeghi, MAS Sadjadi, and RAR Vahdati. Nanoplates controlled synthesis and catalytic activities of silver nanocrystals. Superlattices and Microstructure 46(6):858-863, 2009.

[6] Subramanian Vilayurganapathy, Manjula I Nandasiri, Alan G Joly, Patrick Z El-Khoury, Tamas Varga, Greg Coey, Birgit Schwenzer, Archana Pandey, Asghar Kayani, Wayne P Hess, et al. Silver nanorod arrays for photocathode applications. Applied Physics Letters, 103(16):161112, 2013.

[7] Atsushi Ono, Jun-ichi Kato, and Satoshi Kawata. Subwavelength optical imaging through a metallic nanorod array. *Physical review letters*, 95(26):267407, 200

[50] Nick Kanopoulos, Nagesh Vasanthavada, and Robert L Baker. Design of an image edge detection lter using the sobel operator. Solid-State Circuits, IEEE Journal of, 23(2):358-367,1988.

[17] John Canny. A computational approach to edge detection. Pattern Analysis and Machine Intelligence, IEEE Transactions on, (6):679-698, 1986.

[91] Jianbo Shi and Jitendra Malik. Normalized cuts and image segmentation. Pattern Analysis and Machine Intelligence, IEEE Transactions on, 22(8):888-905, 2000

[36] Stephen Gould, Tianshi Gao, and Daphne Koller. Region-based segmentation and object detection. In *Advances in neural information processing systems*, pages 655–663, 2009

[44] Pedro F Felzenszwalb and Daniel P Huttenlocher. Ecient graph-based image segmentation. International Journal of Computer Vision, 59(2):167- 181, 2004.

[46] Yuri Boykov and Gareth Funka-Lea. Graph cuts and ecient nd image segmentation. Inter-national journal of computer vision, 70(2):109-131, 2006.

[53] Jose M Korathl and A Romagnolig. Separating touching and overlapping objects in particle images–A combined approach. *Chemical Engineering*, 11, 2007

[54] Changming Zhu, Jun Ni, Yanbo Li, and Guochang Gu. General tendencies in segmentation of medical ultrasound images. In Internet Computing for Science and Engineering (ICICSE), 2009 Fourth International Conference on, pages 113-117. IEEE, 2009.

[55] Chunming Li, Chiu-Yen Kao, John C Gore, and Zhaohua Ding. Implicit active contours driven by local binary tting energy. In Computer Vision and Pattern Recognition, 2007. CVPR'07. IEEE Conference on, pages 1-7. IEEE, 2007.

[56] Serge Beucher et al. The watershed transformation applied to image segmentation. *Scanning Microscopy Supplement*, pages 299–299, 1992.

[58] Chunming Li, Chiu-Yen Kao, John C Gore, and Zhaohua Ding. Implicit active contours driven by local binary fitting energy. In *Computer Vision and Pattern Recognition, 2007. CVPR'07. IEEE Conference on*, pages 1–7. IEEE, 2007

[68] Satya P Mallick, Yuanxin Zhu, and David Kriegman. Detecting particles in cryo-EM micrographs using learned features. *Journal of structural biology*, 145(1):52–62, 2004

[85] AM Roseman. Findema fast, efficient program for automatic selection of particles from electron micrographs. *Journal of structural biology*, 145(1):91–99, 2004

[63] Zeyun Yu and Chandrajit Bajaj. Detecting circular and rectangular particles based on geometric feature detection in electron micrographs. *Journal of Structural Biology*, 145(1):168–180, 2004.

[79] Chiwoo Park, Jianhua Z Huang, Jim X Ji, and Yu Ding. Segmentation, inference and classification of partially overlapping nanoparticles. *Pattern Analysis and Machine Intelligence,*
IEEE Transactions on, 35(3):1–1, 2013.

Thanks